

W and Z Boson Production Cross Section Measurements in ATLAS

Verena I. Martinez Outschoorn* on behalf of the ATLAS Collaboration

*Harvard University, 17 Oxford St. Cambridge MA 02138, vimartin@physics.harvard.edu

Abstract. The electroweak boson inclusive production cross sections and their ratios are described in the electron and muon decay channels. The observation of W and Z bosons in the tau decay channel is also presented. The data from pp collisions at 7 TeV were collected during 2010 using the ATLAS detector at the Large Hadron Collider and the results are compared to predictions at NNLO in perturbative QCD.

Keywords: W/Z Production, W Cross Section, Z Cross Section

PACS: 14.70.Fm, 14.70.Hp

INTRODUCTION

Measurements of the production of W and Z bosons probe perturbative QCD predictions, testing the validity of theoretical NNLO calculations and providing information on the parton distribution functions (PDFs). The results presented here [1] constitute an update, with a dataset a hundred times larger, of the initial measurements [2] performed by ATLAS [3]. The uncertainty on the integrated luminosity is reduced from 11% to 3.4% and the results have significantly lower experimental systematic uncertainties. In addition, the $Z \rightarrow ee$ cross section is extended in lepton pseudorapidity (η) from a maximum of 2.47 to 4.9, increasing the range of parton momentum fraction x probed. Measurements of the W and Z cross sections are presented in the electron and muon decay modes. The combination of the electron and muon inclusive cross section results and the W/Z cross section ratio are compared to available predictions based on NNLO QCD using various PDF sets. In addition, the observation of W and Z bosons in the tau decay channel [4, 5, 6] provides a consistency check in the third lepton channel and constitutes a first characterization of an important background to new physics searches.

W AND Z CROSS SECTIONS AND RATIOS IN THE ELECTRON AND MUON CHANNELS

The data were acquired during the LHC runs at $\sqrt{s} = 7$ TeV in 2010, amounting to an integrated luminosity of about 35 pb^{-1} , after requiring a fully operational detector in stable beam conditions. Events were selected for recording and subsequent offline analysis using a three-level single electron or muon trigger. A primary vertex (PV) with at least three tracks serves to select collision candidates. Electron identification is based on a sliding window algorithm forming calorimeter clusters that are then associated to tracks in the Inner Detector (ID). To select $W \rightarrow e\nu$ events, exactly one electron

cluster is required to have transverse energy $E_T > 20$ GeV and to lie within the region where the ID acceptance is matched to the precision measurements of the calorimeter: $|\eta| < 2.47$, excluding the transition region between the barrel and endcap calorimeters $1.37 < |\eta| < 1.52$. The electron is required to satisfy different types of identification (“tight”) criteria to efficiently reject backgrounds from jets. The missing transverse energy (E_T^{miss}) is based on the sum of calorimeter cell energy deposits in topological clusters and is required to be larger than 25 GeV. Further, the transverse mass (m_T) is required to be larger than 40 GeV. For $Z \rightarrow ee$ candidate events, two electrons are required to satisfy the less stringent “medium” identification criteria, have opposite charge and an invariant mass in the range $66 < m_{ee} < 116$ GeV. In the case of $Z \rightarrow ee$ events with an extended range of pseudorapidity, a central electron ($|\eta| < 2.47$) passing the “tight” criteria is required and another electron has to be reconstructed in the forward region ($2.5 < |\eta| < 4.9$). The forward region extends beyond the ID coverage, so the electron identification is based on calorimeter cluster shapes alone.

Muon identification is based on combined tracking using both the ID and the muon spectrometer. Combined tracks with transverse momentum $p_T > 20$ GeV are selected within $|\eta| < 2.4$. Cosmic ray contamination is reduced with pointing requirements to the PV in the center of the detector. Muons from heavy quark decays are removed with an isolation requirement relative to the muon p_T of $\Sigma p_T^{\text{ID}}/p_T < 0.2$, where the ID tracks are in a cone in $\eta - \phi$ space of radius 0.4 around the muon. $W \rightarrow \mu\nu$ candidate events are selected requiring the E_T^{miss} , determined from calorimeter and muon tracking information, to be larger than 25 GeV and $m_T > 40$ GeV. For $Z \rightarrow \mu\mu$ candidate events, two muons are required to be of opposite charge and have an invariant mass in the range $66 < m_{\mu\mu} < 116$ GeV.

The candidate sample size for each lepton channel is about 130,000 for W and 10,000 for Z , with an additional 4,000 forward $Z \rightarrow ee$ events. The electroweak background contributions to W and Z are obtained from Monte Carlo simulation scaled to the NNLO cross section. The main background contributions to W arise from $W \rightarrow \tau\nu$ (2.8%), where the τ decays leptonically, and additionally in the muon channel from $Z \rightarrow \mu\mu$ events, where one of the muons falls outside of the acceptance (3.5%). The electroweak background contributions to $Z \rightarrow ee$ and $Z \rightarrow \mu\mu$ are small (0.3% and 0.1% respectively), as are the diboson contributions (0.2%). The background from jets produced via QCD processes (referred to as “QCD background”) is derived from fits comparing the E_T^{miss} (for W) or the invariant mass (for Z) distributions in data and in templates derived from simulation. The resulting predictions are of 2–4% for the electron channel analyses, except for the case of the forward $Z \rightarrow ee$ selection (27%), where W s in association with jets faking a forward electron provide an additional background. The QCD background in the muon channel is estimated from extrapolations from control regions, yielding contributions of 1.7% for $W \rightarrow \mu\nu$ and 0.2% for $Z \rightarrow \mu\mu$.

The total W and Z cross section times branching ratio is measured using a “cut-and-count” method, whereby candidate events are selected in data, the number of expected background events is subtracted and the signal yield is divided by the integrated luminosity corresponding to the run selections and trigger employed. This result is corrected for acceptances and detector effects. Measurements of the integrated cross sections within the fiducial regions, providing the most precise experimental results for comparison to theory, and after extrapolation to the full kinematic region can be found in [1] for the

electron and muon channels. The total inclusive cross sections are consistent for the two decay modes within their measurement uncertainties. The combination of both channels is shown in Table 1 and Figure 1, assuming the two lepton decay mode cross sections to be independent, with the exception of the common parts in the acceptance calculation, the E_T^{miss} uncertainty in the W channels and the luminosity uncertainty that are treated as fully correlated.

TABLE 1. Total averaged cross sections times leptonic branching ratios in nb for W^+ , W^- , W and Z/γ^* production in the combined electron and muon final states. The uncertainties denote the statistical, experimental systematic, luminosity and acceptance errors. The ratios of the cross sections times leptonic branching fractions are also shown with their corresponding statistical, experimental systematic and acceptance uncertainties. Theoretical predictions for one choice of PDF set [7] at NNLO in perturbative QCD are included for comparison, showing the PDF uncertainties only, taken at 68% C.L.

Process	Combined Measurement	MSTW08
$\sigma_{W^+}^{\text{tot}} \cdot \text{BR}(W \rightarrow l\nu)$ [nb]	$6.257 \pm 0.017 \pm 0.152 \pm 0.213 \pm 0.188$	6.16 ± 0.11
$\sigma_{W^-}^{\text{tot}} \cdot \text{BR}(W \rightarrow l\nu)$ [nb]	$4.149 \pm 0.014 \pm 0.102 \pm 0.141 \pm 0.124$	4.30 ± 0.08
$\sigma_W^{\text{tot}} \cdot \text{BR}(W \rightarrow l\nu)$ [nb]	$10.391 \pm 0.022 \pm 0.238 \pm 0.353 \pm 0.312$	10.46 ± 0.18
$\sigma_{Z/\gamma^*}^{\text{tot}} \cdot \text{BR}(Z/\gamma^* \rightarrow ll)$ [nb]	$0.945 \pm 0.006 \pm 0.011 \pm 0.032 \pm 0.038$	0.964 ± 0.018
$\sigma_{W^+}^{\text{tot}} \cdot \text{BR}/\sigma_Z^{\text{tot}} \cdot \text{BR}$	$6.563 \pm 0.049 \pm 0.134 \pm 0.098$	6.388 ± 0.026
$\sigma_{W^-}^{\text{tot}} \cdot \text{BR}/\sigma_Z^{\text{tot}} \cdot \text{BR}$	$4.345 \pm 0.034 \pm 0.095 \pm 0.065$	4.459 ± 0.018
$\sigma_W^{\text{tot}} \cdot \text{BR}/\sigma_Z^{\text{tot}} \cdot \text{BR}$	$10.906 \pm 0.079 \pm 0.215 \pm 0.164$	10.85 ± 0.018

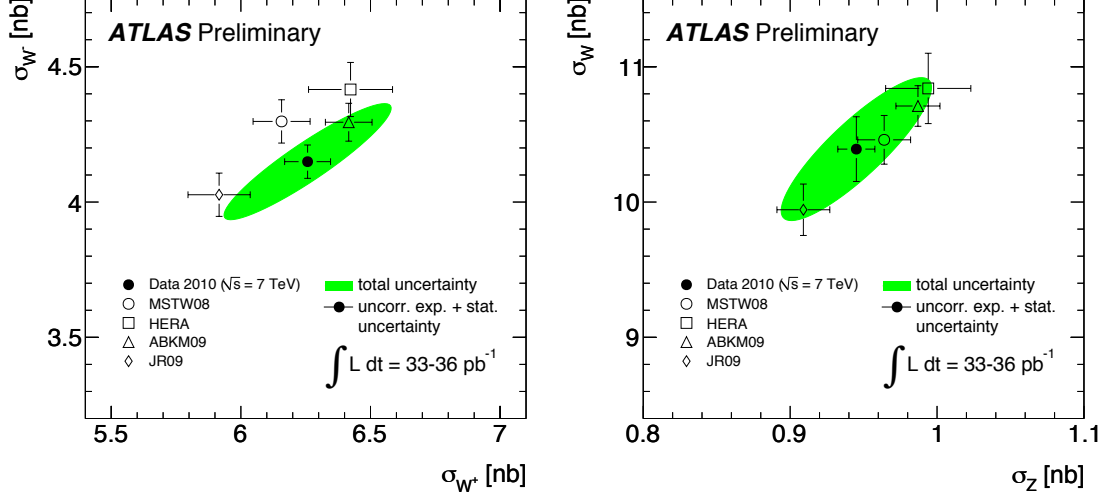


FIGURE 1. Measured and predicted cross sections times leptonic branching ratios, for σ_{W^-} vs. σ_{W^+} (left) and $(\sigma_{W^+} + \sigma_{W^-})$ vs. σ_{Z/γ^*} (right). The correlations between the various cross sections are accounted for and the projections of the ellipse to the axes correspond to one standard deviation uncertainty of the cross sections. Theoretical predictions are calculated to NNLO in QCD using PDFs by the MSTW [7], ABKM [8, 9], HERA [10, 11] and JR [12] groups. Only the PDF uncertainties on the theoretical predictions are shown.

Compared to the first measurement in ATLAS [2], the statistical uncertainty of the total cross-section measurement is improved to the level of $< 1\%$, the systematic uncertainty by a factor of about three, to 2.4% and 1.2% for the W and Z cross sections

respectively, and the luminosity uncertainty by a factor of four to 3.4%. The $W \rightarrow e\nu$ cross sections are measured with an experimental uncertainty of 2.8% to 3.0% for the two charges, which contains approximately equal contributions from the combined electron efficiency and the missing transverse energy. The central $Z \rightarrow ee$ cross section is measured with an experimental precision of 3.5%, dominated by the uncertainty of the reconstruction efficiency measurement. The $Z \rightarrow ee$ using the forward selection has an experimental precision of about 10%. Within their uncertainties the central and forward Z results are compatible. The $W \rightarrow \mu\nu$ cross section is measured with an experimental uncertainty of 2.4% and of 2.7% for W^+ and W^- respectively, also dominated by the contribution from the calorimeter E_T^{miss} scale and resolution (2%). The $Z \rightarrow \mu\mu$ cross section is measured with an experimental precision of 1.1%, mainly arising from the reconstruction efficiency uncertainty. The uncertainty on the theoretical extrapolation from the fiducial region of the measurement to the total phase space is 3.0% and 4.0% in the W and Z measurements respectively [2]. The cross section results in Figure 1 are compared with predictions from four sets of NNLO parton distributions, showing consistency of all NNLO predictions within the total accuracy of the measurement of about 5%. The ratios of the measured W and Z cross sections are also listed in Table 1, accounting for the correlations of errors. The uncertainty on these ratios (2.7% for W/Z) is smaller than that on the cross sections due to cancellations in the ratios and the results are also consistent with NNLO predictions.

W AND Z OBSERVATION IN THE TAU CHANNEL

The first observation of $W \rightarrow \tau\nu$ events with a hadronic τ candidate and large E_T^{miss} has been performed with a dataset corresponding to 546 nb^{-1} of integrated luminosity [4]. In addition, $Z \rightarrow \tau\tau$ events have been observed in three decay channels: the dilepton decay mode $Z \rightarrow \tau\tau \rightarrow e\mu + 4\nu$ using a dataset of 35 pb^{-1} [5] and in the lepton-hadron decay modes including a soft electron or muon, using 8.3 pb^{-1} and 8.5 pb^{-1} of integrated luminosity, respectively [6]. The signal yields are in agreement with Standard Model expectations for all W and Z analyses.

REFERENCES

1. The ATLAS Collaboration, ATLAS Conference Note, ATLAS-CONF-2011-041, 2011.
2. The ATLAS Collaboration, *JHEP* **12**, 060 (2010).
3. The ATLAS Collaboration, *JINST* **3**, S08003 (2008).
4. The ATLAS Collaboration, ATLAS Conference Note, ATLAS-CONF-2010-097, 2010.
5. The ATLAS Collaboration, ATLAS Conference Note, ATLAS-CONF-2011-045, 2011.
6. The ATLAS Collaboration, ATLAS Conference Note, ATLAS-CONF-2011-010, 2011.
7. A. D. Martin, W. J. Stirling, R. S. Thorne, and G. Watt, *Eur. Phys. J.* **C63**, 189–285 (2009).
8. S. Alekhin, J. Blumlein, S. Klein, and S. Moch, *Phys. Rev.* **D81**, 014032 (2010).
9. S. Alekhin, J. Blumlein, and S.-O. Moch, *PoS DIS2010*, 021 (2010).
10. The H1 and ZEUS Collaboration, *JHEP* **01**, 109 (2010).
11. The H1 and ZEUS Collaboration, H1prelim-10-044/ZEUS-prel-10-008, 2010 and V. Radescu, *PoS ICHEP*, 168 (2010).
12. P. Jimenez-Delgado and E. Reya, *Phys. Rev.* **D79**, 074023 (2009).

Copyright CERN for the benefit of the ATLAS collaboration